Geological and Geochemical Characteristics of the Terrestrial Lower Jurassic Shale in Tarim Basin and its Favorable Exploration Areas

Qifeng Wang*, Haifa Tang*, Zhi Guo, Gang Cheng, Zhikai Lv and Qunming Liu

Research Institute of Petroleum Exploration and Development, PetroChina, Beijing, China

Large amounts of conventional gas resources that originated from terrestrial Lower Jurassic shale were discovered in the Tarim Basin, indicating promising exploration prospects for shale gas resources, whereas limited understandings were obtained on the geological and geochemical characteristics of the Lower Jurassic shale. In this study, based on cores of exploration wells and field outcrops, total organic carbon (TOC) pyrolysis, microscopic composition, organic elements, vitrinite reflectance, x-ray diffraction, and methane isothermal adsorption experiments were carried out on Lower Jurassic shale in the Tarim Basin. The results show that the TOC content of shale is relatively high, but the TOC content of shale in different regions is quite different. Among them, the Kuqa Depression is the highest (more than 3%), the Southwest Tarim Basin is second (more than 1%), and the East Tarim Basin is the lowest. The main types of kerogen in shale are mainly type III and type II_2. The thermal evolution maturity of shale in different regions is quite different; the highest Ro of shale in the Southwest Tarim Basin is more than 2.0% and that of shale in the Kuqa depression is higher than 1.5%, both of which have entered the stage of high-over-mature evolution, and the shale in the East Tarim Basin is only in the low maturity–mature stage. The overall content of brittle minerals such as quartz in shale is greater than 40%, which has good fracturing properties. The adsorbed gas content of shale is high, but there is a great difference ($0.5–4 \, m^3/t$), which is related to the large difference in the abundance of organic matter, thermal maturity, and clay mineral content of shale. Therefore, the Lower Jurassic shale gas in the Tarim Basin has good prospects for exploration. Based on the superposition method of the main controlling geological factors, it is predicted that the favorable areas for shale gas exploration are mainly located in the Keshen and Yinan-Yeyun areas of the Kuqa Depression and the Caohu Sag-Mandong area of the East Tarim Basin. This research not only provides basic data for the evaluation of shale gas resources in our country, but also provides certain guidance for the exploration of Lower Jurassic shale gas in the Tarim Basin.

Keywords: terrestrial shale gas, geological characteristic, geochemical characteristic, favorable exploration area, lower Jurassic shale, Tarim Basin

INTRODUCTION

As conventional oil and gas resources are increasingly scarce, the main energy status of oil and gas mainly benefits from the contribution of shale oil and gas (Hughes, 2013; Hopkins, 2017); in particular, shale gas provides a realistic possibility for coping with climate change and sustainable development of low-carbon economy (Zou, 2017; Hu et al., 2021). In recent years, with the successful development of shale gas in North America (Montgomery et al., 2005; Zou, 2017), the related research on shale gas in China has also been carried out rapidly, but mainly concentrated in the lower Paleozoic marine shale in the Sichuan Basin (Pu et al., 2010; Zou et al., 2010; Haikuan et al., 2011; Jiang et al., 2012; Hu et a., 2018). The Tarim Basin is the largest petroliferous basin in China. Many rounds of oil and gas resource evaluation and oil and gas drilling have confirmed that it has huge conventional oil and gas resources (Chen et al., 1998; Li et al., 2000; Zhao and Zhang, 2002; Gao et al., 2013), which also indicates that it has great shale gas resource potential (Gao et al., 2013; Jiang et al., 2018; Jiang et al., 2019).

The lower Jurassic shale in the Tarim Basin is a set of fine-grained sediments, which are mainly deposited in lacustrine and swamp environments. In the past, it has been studied as the source rock of conventional oil and gas (Chen et al., 1998; Li et al., 2000; Zhao and Zhang, 2002; Gao et al., 2013). In recent years, some scholars have carried out research on Jurassic shale gas in the Tarim Basin, but most of them focus on the reservoir structure (Gao et al., 2013; Xiao et al., 2014) and adsorption characteristics (Gao et al., 2015), or mostly concentrated in some areas of the Tarim Basin (Jiang et al., 2018; Jiang et al., 2019), and fail to point out the future shale gas exploration direction from the perspective of the whole basin.

Firstly, based on shale cores obtained from exploration wells and field outcrops, this research has carried out a series of experiments, which included total organic carbon (TOC) pyrolysis, microscopic composition analysis, organic elements, vitrinite reflectivity, x-ray diffraction, and methane isothermal adsorption to analyze the geological and geological characteristics of shale. Then, combined with the division of shale strata in single wells, lateral distribution of cross-well profile, seismic inversion, sedimentary facies, and structure contour data, we analyzed the structural burial depth, TOC content, and Ro plane distribution characteristics of the shale. Finally, using the superposition method of the main controlling geological factors, the exploration prospects and favorable areas of the Lower Jurassic shale gas in the Tarim Basin are predicted. This study not only provides reliable basic data for shale gas resource evaluation in China, but also plays a guiding role in shale gas exploration of Lower Jurassic in the Tarim Basin.

GEOLOGICAL BACKGROUND

The Tarim Basin is located at the western end of the North China-Tarim platform; the north is adjacent to the Tianshan fold belt, and the southwest is bounded by the Kunlun fold belt and is separated from the Qaidam Basin by the Altyn fault to the southeast. The exploration area is about 560,000 km^2, which is the largest Mesozoic and Cenozoic inland sedimentary basin in China (Jia, 1997). The Tarim Basin includes seven first-level structural units including the Kuqa Depression, Northern Uplift, Northern Depression, Central Uplift, Southwest Depression, Southern Uplift, and Southeast Depression (**Figures 1A,B**). Since the Sinian, the Tarim Basin has experienced a complete depositional cycle from marine facies, marine-terrestrial transitional facies, to continental facies (He et al., 2005), with a thickness of 18,000 m. The Lower Jurassic is dominated by gray-green, gray, and dark purple sandstone and mudstone, and is composed of delta, shallow lake, semi-deep lake, and swamp facies (Gao et al., 2013) (**Figure 1C**).

METHODS

The sample preparation and test procedures for TOC, pyrolysis, maceral, elemental composition, vitrinite reflectance, x-ray diffraction, and isothermal adsorption were the same with Jiang et al. (2017).

RESULTS AND DISCUSSION

Distribution and Thickness

According to the statistics of the single-well burial depth of the effective shale of the Lower Jurassic in the Tarim Basin, combined with the seismic inversion data, structural morphology and depositional environment of the areas without wells, or lack of well drilling, the burial depth of the Lower Jurassic shale is determined. The burial depth contour map of the Lower Jurassic shale in the Tarim Basin was drawn (**Figure 2A**). The results show that the Lower Jurassic shale in the Tarim Basin is mainly distributed in the Kuqa Depression, East Tarim, and Southwest Tarim. The maximum buried depth is located in the central area of Baicheng Sag and Yangxia Sag in the Kuqa Depression, reaching more than 7,000 m. The buried depth of the Caohu Sag in the East Tarim Basin is mostly about 5,000 m, and the burial depth gradually goes southeast (the East Tarim Basin) and decreases. The burial depth in the southwestern part of the Tarim Basin is relatively shallow, only some areas near Zepu exceed 5,000 m, and most of the other areas are below 5000 m.

Based on a comprehensive analysis of single-well shale interval division, lateral distribution of continuous well profiles, seismic inversion data, and sedimentary facies data, the contour map of the cumulative thickness of the Lower Jurassic shale in the Tarim Basin was drawn (**Figure 2B**). The results show that the Lower Jurassic shale is mainly distributed in the Kuqa Depression, the Southwest Tarim, and the East Tarim. Among them, the shale in the Kuqa Depression and the Southwest Tarim is relatively thick, and the thickness center is located in Yangxia, Kuqa Depression. The maximum thickness of the Kashi sag and Yecheng sag in the southwestern part of the Tarim Basin reaches 200 and 100 m respectively. On the whole, the thickness of the shale gradually decreases from the center of the depression to the surrounding area until it pinches out.
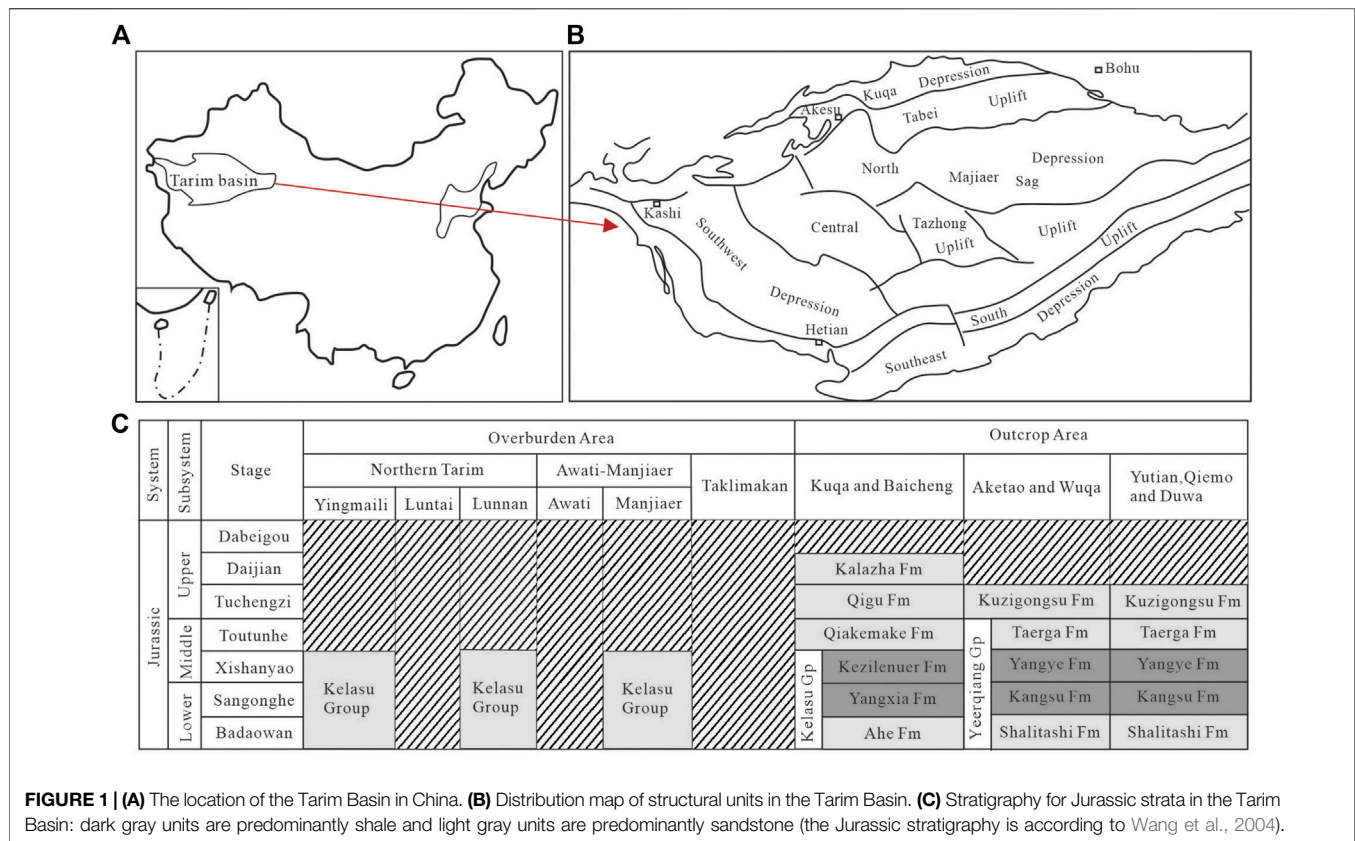
FIGURE 1 | (A) The location of the Tarim Basin in China. (B) Distribution map of structural units in the Tarim Basin. (C) Stratigraphy for Jurassic strata in the Tarim Basin: dark gray units are predominantly shale and light gray units are predominantly sandstone (the Jurassic stratigraphy is according to Wang et al., 2004).

Organic Matter Richness

TOC and hydrocarbon generation potential (PG) are effective indicators for evaluating the organic matter richness of shale (Peters and Cassa, 1994; Hu et al., 2018). The results of tests show that the abundance of organic matter in shale in different regions of the Tarim Basin is quite different. The TOC of the Lower Jurassic shale in the Kuqa Depression is generally high, mostly ranging from 1.5% to 3%, up to 6%, and that of most carbonaceous mudstone is more than 10%. Among them, the TOC of Kezi 1 shale is between 2% and 15%, with an average of about 10%, and the PG is between 0.2 and 0.5 mg/g (Figure 3A); the TOC of Yixi 1 shale is between 5% and 25%, the average is about 10%, and PG is between 3 and 10 mg/g (Figure 3B).

Compared with the Kuqa Depression, the organic matter abundance of the Lower Jurassic shale in the Eastern Tarim Basin is generally lower, the TOC is mostly between 0.5% and 2%, and PG is mainly between 0.93 and 3.76 mg/g, but mostly less than 2.0 mg/g. However, the shale of well Huayingcan 1 is rich in organic matter, with TOC content mostly between 0.5% and 4%, and PG between 1.5 and 6 mg/g (Figure 3C). The abundance of organic matter in the Lower Jurassic shale in the southwestern Tarim basin is relatively high.
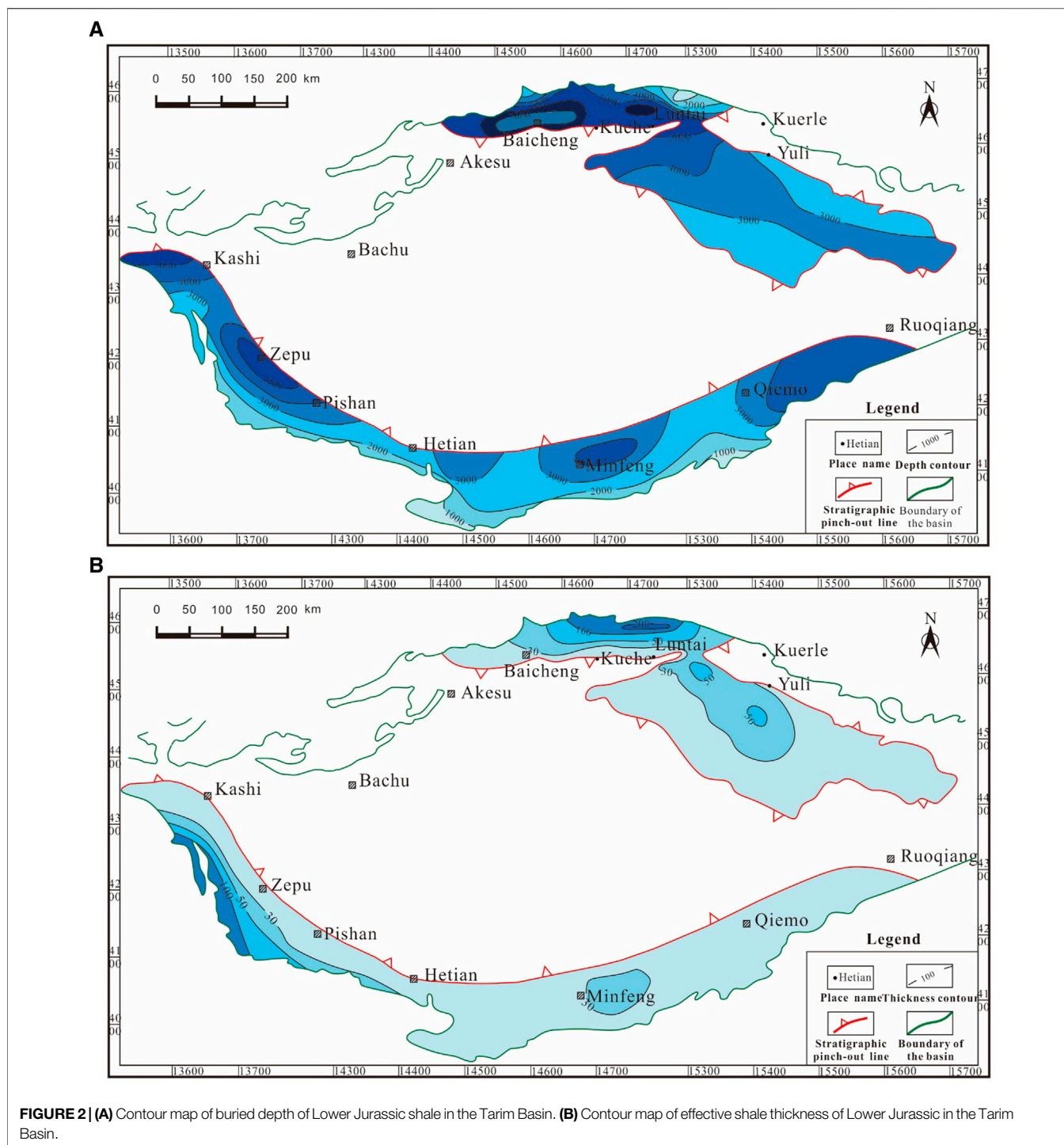
The Tarim Basin is relatively high. However, due to the lack of core samples, this research analyzed several shale samples from field profiles in this area (Figure 3D), and most of their TOC content is greater than 1%, the maximum is over 5%, and maximum PG can reach 2.5 mg/g. However, the TOC of shale samples from different field profiles is different. The lowest TOC of the Lower Jurassic shale in the Kushanhe section is 1.3%, and the TOC of the shale in the Mogan section and the Heshirap section can exceed 5%.

Based on the analysis of core and field outcrop test data, combined with the TOC data predicted by logging data, the TOC contour plane distribution of the Lower Jurassic shale in the Tarim Basin is carried out. The results show that the TOC of the Lower Jurassic shale in the Tarim Basin is generally higher. Among them, the TOC of the shale in the Baicheng Sag–Yangxia Sag of the Kuqa Depression exceeds 3%. The TOC of the shale in the East Tarim area is more than 1%, and the high value is mainly located in the Caohu Sag-Mandong area and Yingjisu Sag area. The TOC of some shale in the Southwest Tarim Basin is greater than 1.5% (Figure 4).

Organic Matter Type

Generally, the maceral content of organic matter, H/C-O/C chart, and HI-Tmax chart can be used to evaluate the organic matter type of shale (Tissot and Welte, 1984; Hu et al., 2016). The results of tests and analysis show that the organic matter of the Lower Jurassic shale in the Kuqa Depression and Southwest Tarim Basin is dominated by vitrinite and inertinite, while the content of saprolite and chitin is relatively low, which is characterized by type II_2 and type III organic matter (Figure 5A). At the same time, the H/C-O/C chart and HI-Tmax chart both show that shale is dominated by type III kerogen, followed by type II_2

FIGURE 2 | (A) Contour map of buried depth of Lower Jurassic shale in the Tarim Basin. (B) Contour map of effective shale thickness of Lower Jurassic in the Tarim Basin.

kerogen, and type II_1 and type I kerogen are almost underdeveloped (**Figures 5B,C**).

Thermal Maturity

Vitrinite reflectance (Ro) is an effective indicator for evaluating the thermal maturity of shale (Peters and Cassa, 1994). The results of tests and analysis show that the Ro of the Jurassic shale in Well Yixi 1 in the Kuqa Depression is 1.01%–1.19%

(burial depth of 3,040–3,530 m), with an average value of 1.12%. The evolution of organic matter is at a mature stage. The value of Ro increases with the burial depth, and there is a good linear correlation between them (**Figure 6**). The Ro of the Jurassic shale in Well Yinan 2 in the Kuqa Depression is between 0.57% and 0.85% (burial depth of 4,249–4279 m), with an average value of 0.73%. The evolution of organic matter is at a mature stage, and there is also a good linear relationship between Ro and burial
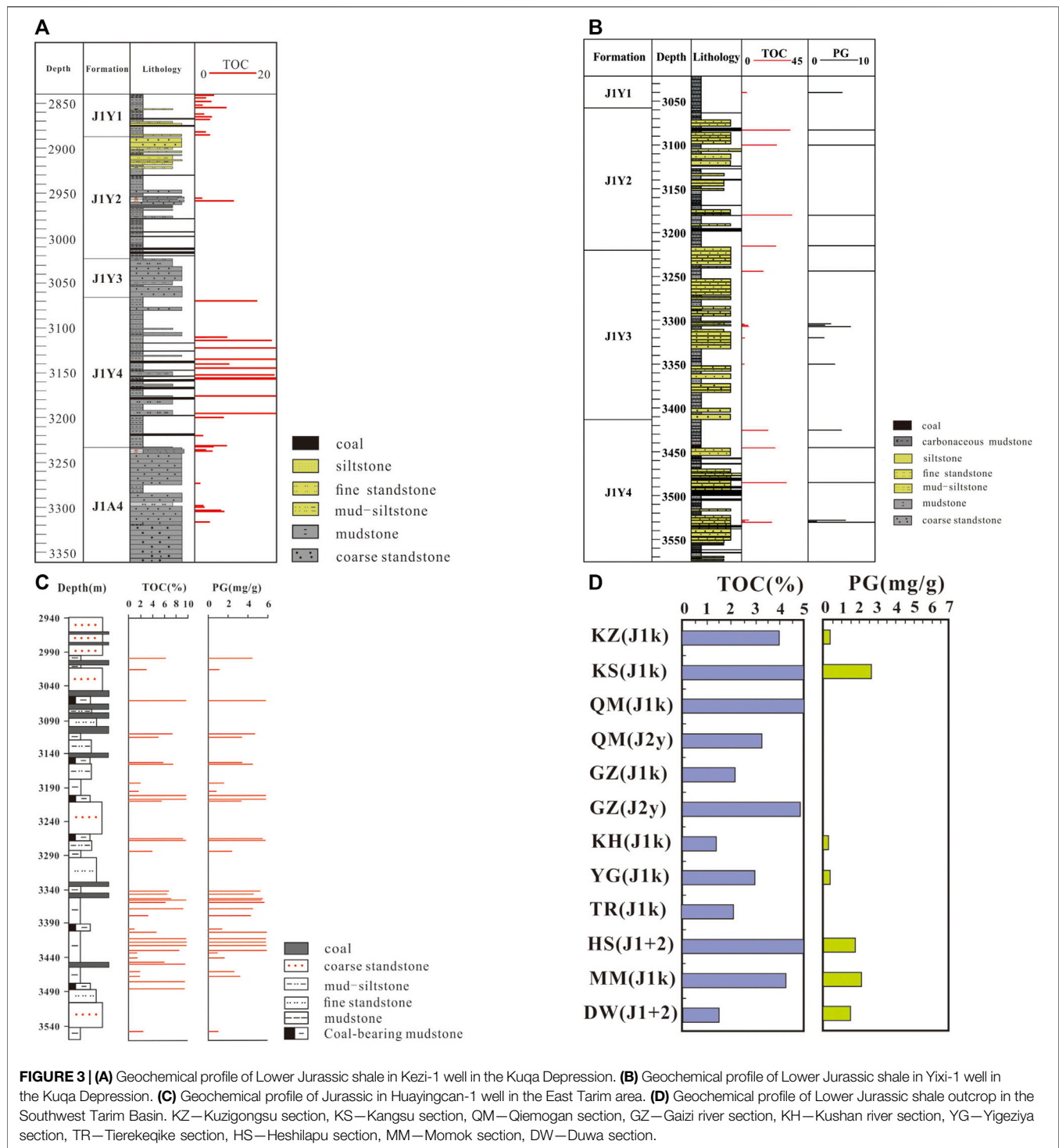
FIGURE 3 | (A) Geochemical profile of Lower Jurassic shale in Kezi-1 well in the Kuqa Depression. (B) Geochemical profile of Lower Jurassic shale in Yixi-1 well in the Kuqa Depression. (C) Geochemical profile of Jurassic in Huayingcan-1 well in the East Tarim area. (D) Geochemical profile of Lower Jurassic shale outcrop in the Southwest Tarim Basin. KZ—Kuzigongsu section, KS—Kangsu section, QM—Qiemogan section, GZ—Gaizi river section, KH—Kushan river section, YG—Yigeziya section, TR—Tierekeqike section, HS—Heshilapu section, MM—Momok section, DW—Duwa section.

depth (**Figure 6**). In contrast, the burial depth of the lower Jurassic shale in Well Yixi 1 is less than that of Well Yinan 2, while Ro is larger than that of Well Yinan 2. This is mainly related to the thermal effect caused by strong structural compression stress (Zhang et al., 2007). The Ro of the Lower Jurassic shale at the Kuzigongsu section in the Southwest Tarim Basin is between 1.3% and 1.8%, and is currently at a high maturity stage; the Ro of

the shale at the Kangsu section is between 0.5% and 1.0%, which is in the low maturity–mature stage. The average Ro of the shale in Yigeziya section is 1.15%, which is in the mature stage. In general, the Lower Jurassic shale in the Southwest Tarim Basin is in a mature stage.

Based on the analysis of core and field outcrop test data, the relationship between Ro and burial depth of shale in different
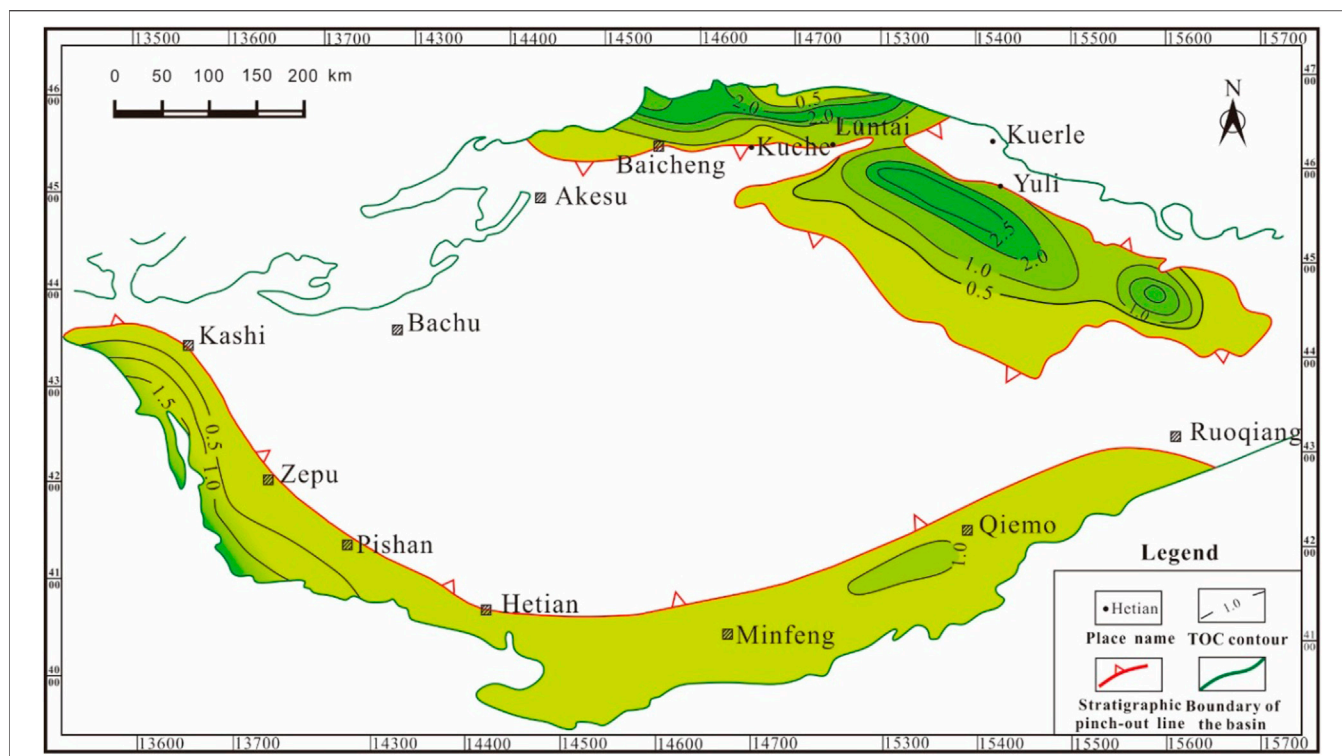
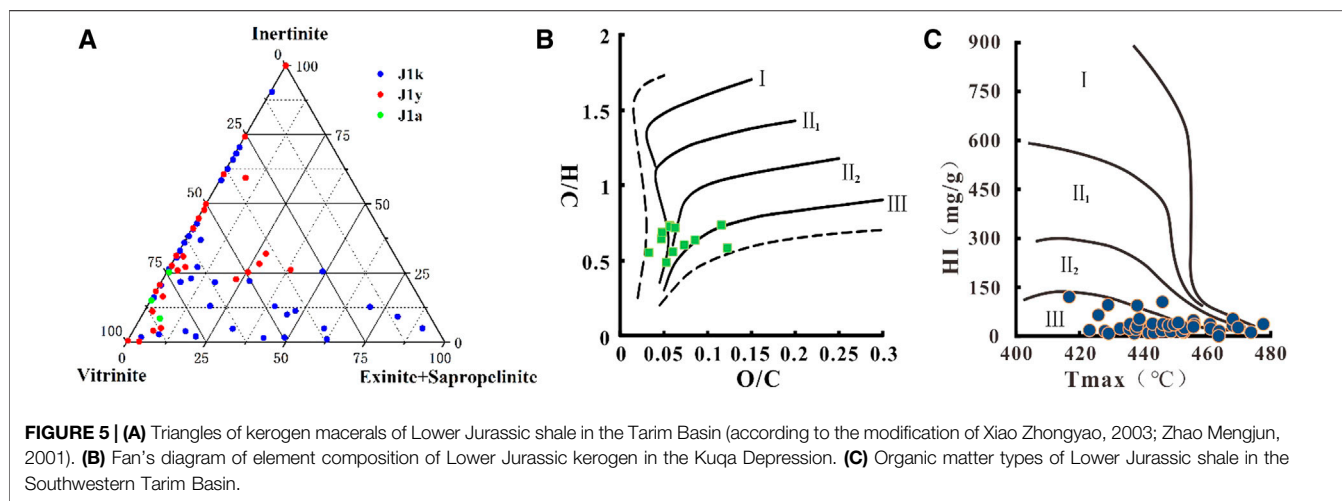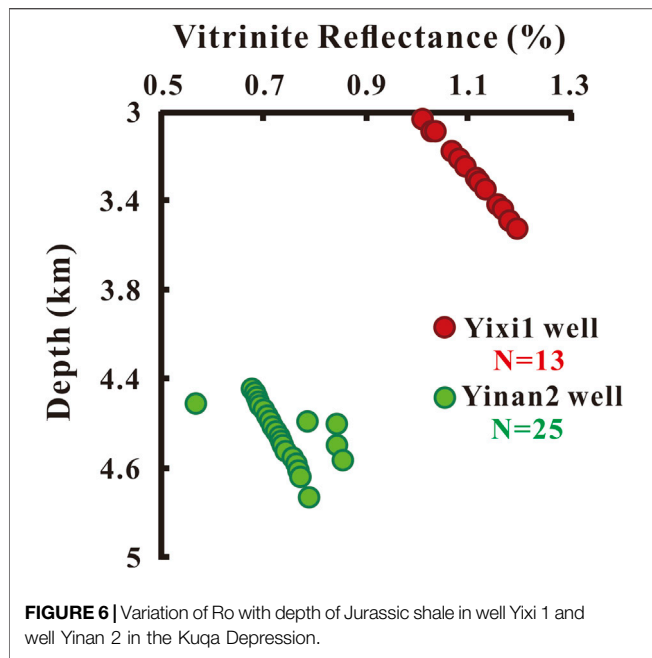**FIGURE 4 |** Contour map of TOC of Lower Jurassic in the Tarim Basin.

FIGURE 5 | (A) Triangles of kerogen macerals of Lower Jurassic shale in the Tarim Basin (according to the modification of Xiao Zhongyao, 2003; Zhao Mengjun, 2001). **(B)** Fan's diagram of element composition of Lower Jurassic kerogen in the Kuqa Depression. **(C)** Organic matter types of Lower Jurassic shale in the Southwestern Tarim Basin.

regions has been established, and combined with the tectonic burial depth of the Lower Jurassic shale in the Tarim Basin, the Ro plane distribution of lower Jurassic shale in the Tarim Basin was carried out. The results show that the thermal evolution maturity of organic matter in the Lower Jurassic shale is relatively high in the Baicheng Sag in the Kuqa Depression, and Kashgar Sag and Yecheng Sag in the Southwest Tarim Basin, with a Ro of more than 2%, which is at a high-over-mature stage. Among them, the maximum buried depth of the Jurassic in the center of Baicheng Depression exceeds 7,000 m, and its Ro is

predicted to be as high as 2.2%–2.5%. In contrast, the thermal evolution degree of the East Tarim Basin is relatively low due to the relatively shallow buried depth, and Ro is mostly less than 1% (**Figure 7**).

Hydrocarbon Generation History

The Tarim Basin has been in a subsidence state since the Mesozoic. However, the subsidence rate and geothermal gradient of the Lower Jurassic strata are different in different structural units (He et al., 2005; Qiu et al., 2015), especially the Kuqa Depression, the Southwest

FIGURE 6 | Variation of Ro with depth of Jurassic shale in well Yixi 1 and well Yinan 2 in the Kuqa Depression.

Tarim, and other piedmont depressions that are affected by strongly tectonic movement. Due to the influence of movement, the structural strength of different regions is different, leading to obvious differences in the hydrocarbon generation and evolution of shale in different regions.

Since the Mesozoic, the Kuqa Depression has experienced the Yanshan Movement and the Himalayan Movement (Tang et al., 2008), leading to long-term shallow burial of the Lower Jurassic shale from the Jurassic to Tertiary, and the tectonic evolution process of short-term deep burial from Neogene to Quaternary (**Figure 8A**). At the same time, the geothermal gradient in the Kuqa Depression has gradually decreased since the Jurassic, from 2.3°C/100 m in the Mesozoic to 2.0°C/100 m at present (Li et al., 2000; Wang et al., 2002). Specifically, from the end of Jurassic to the early Cretaceous (early Yanshan: 150–135 Ma), the Lower Jurassic shale began to enter the hydrocarbon generation threshold (Ro = 0.5%). After that, the Jurassic shale has been in a stable shallow burial stage throughout the Yanshan period, with a buried depth of less than 3,000 m, and the organic matter is in a low-mature stage. Until the early Neogene (Early Himalayan period: 25–20 Ma), the Jurassic shale entered mature stage. Since then, under the influence of the Himalayan movement, shale has entered a stage of rapid deep burial. In the middle of the Neogene (Middle Himalayan: 10 Ma), the shale has entered a stage of high maturity (Ro = 1.2%) (**Figure 8A**).

The Southwest Tarim has been in an extensional environment for a long time since the Mesozoic (Pan and Hu, 2020), and the burial rate of the Lower Jurassic shale can reach up to 42.9–57.1 m/Ma. Under the influence of the Yanshan Movement, the burial rate of the Late Cretaceous slowed down. During this process, the geothermal gradient gradually decreased from 2.8°C/100 m, and by the late Neogene, the overall formation was uplifted, and the geothermal gradient dropped to 2.1°C/100 m (Li et al., 2000). Specifically, the

Lower Jurassic shale entered the low-maturity stage in the middle Cretaceous, after which the burial rate decreased, and did not enter the mature stage.

Ro = 0.7% until the end of the Paleogene. In the middle and late Neogene, the Lower Jurassic shale reached a high maturity stage (Ro = 1.2%). Since the Pleistocene, the thermal evolution of the Lower Jurassic shale has ceased due to the uplift and denudation of the formation due to structural uplift (**Figure 8B**). In fact, due to differences in the burial evolution of shale in different areas of the Southwest Tarim, the current thermal evolution of shale in different areas is different. Among them, the Kuzi Gongsu section and Yigeziya section have entered the mature stage, while the Kangsu section, Yangye section, and Duwa section shale are still in the immature–low mature stage.

The subsidence rate of the Lower Jurassic shale in the northeast Tarim Basin is much lower than that of the Kuqa Depression and the Southwest Tarim Basin. Because there are many depressions, elevations, and slopes in the northeast of the Tarim Basin, and the subsidence amplitudes in different regions are different, the thermal evolution history of shale in different regions is also different. Taking the Korla nose-shaped bulge-Kongque River slope area as an example, the Lower Jurassic shale was in a state of continuous subsidence during the Early-Middle Jurassic. At this time, the geothermal gradient was 2.3°C/100 m, and then in the Late Jurassic (Yanshan Late period) experienced a large uplift and continued subsidence after the Cretaceous. Since the Neogene, the Lower Jurassic shale has been buried rapidly and deeply, with a maximum subsidence rate of 146 m/Ma, and a geothermal gradient to 1.9°C/100 m. It was not until the mid-Neogene that the Lower Jurassic shale entered the low maturity–mature stage (**Figure 8C**).

Compared with the Kuqa Depression and the Southwest and the Northeast Tarim Basin, the Lower Jurassic shale subsidence in the Southeast Tarim Basin is the smallest, and most of the areas are still less than 3000 m. The subsidence rate is also relatively slow, the Jurassic-Cretaceous subsidence rate is about 10 m/Ma, the Paleogene subsidence rate increased to 20 m/Ma, and the Neogene-Quaternary subsidence rate further increased to 30 m/Ma. However, due to the relatively small burial depth and low geothermal gradient, most areas in the southeast of Tajikistan are still in the immature stage, and only the deeply buried Lower Jurassic shale entered the low maturity–mature stage at the end of the Paleogene (**Figure 8D**).

Mineralogy

Shale not only has the ability to generate gas, but also serves as an effective reservoir for natural gas. The mineral composition of shale determines its fracturing effect in the later development process. The higher the content of brittle minerals, the better the fracturing effect, which is more conducive to the development and utilization of shale gas (Loucks and Ruppel, 2007). XRD analysis test results show that the lower Jurassic shale in the Tarim Basin is dominated by clay minerals and brittle minerals such as quartz, feldspar, and calcite. The content of other minerals is mostly less than 20%. Specifically, the clay mineral
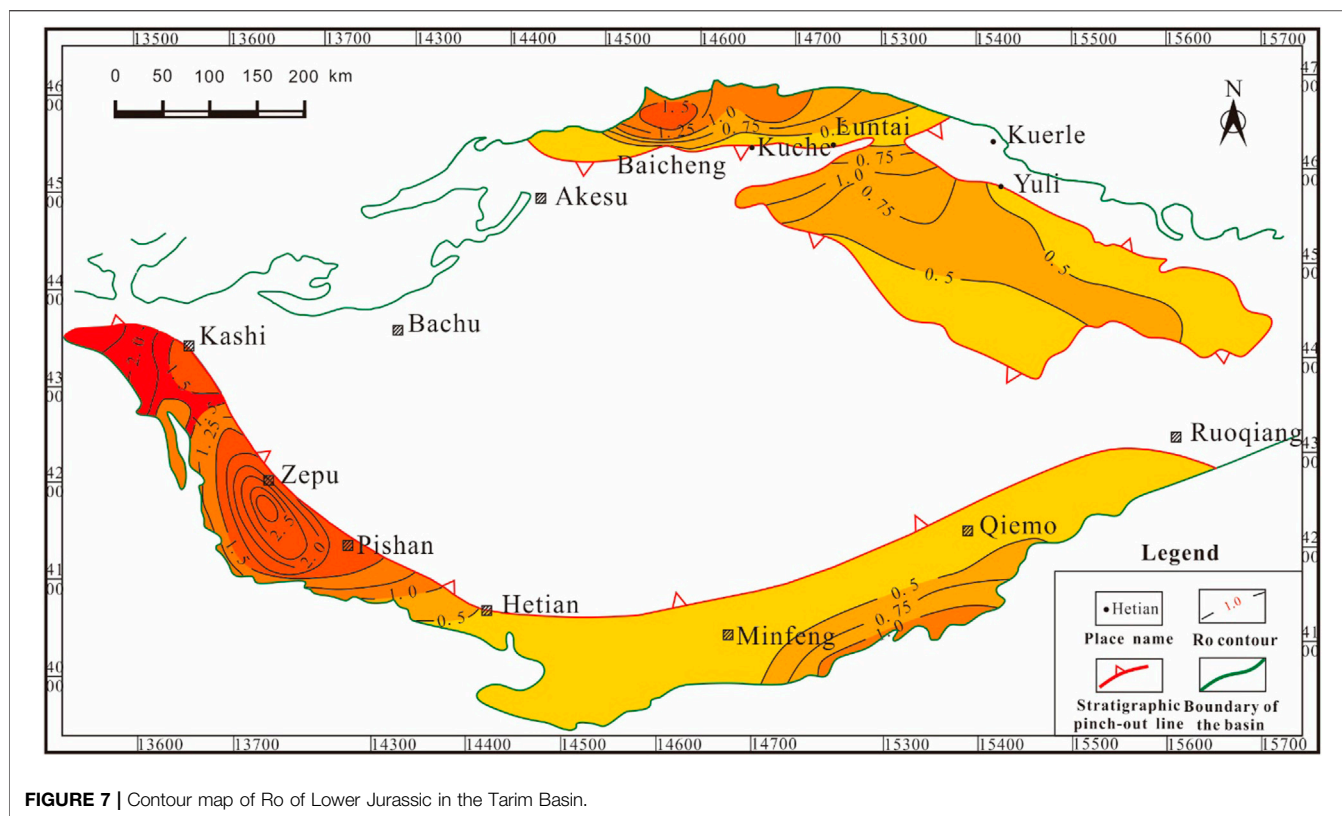
FIGURE 7 | Contour map of Ro of Lower Jurassic in the Tarim Basin.

content is 30%–72%, mostly more than 40%, and the average content is about 51.14%. The quartz content is mostly 18%–62%, and the average content is about 40.83%. The feldspar content is mostly less than 5%. A certain content of pyrite and siderite reflects a strong reducing sedimentary environment. Among them, the main content of brittle minerals such as quartz, feldspar, and calcite is between 28% and 67%, and the average content is about 44.08% (**Figure 9**).

On the whole, the mineral composition of shale in the study area is dominated by brittle minerals such as quartz and clay minerals, among which the content of brittle minerals is more than 40%, which is conducive to the later fracturing development. The content of clay minerals is more than 40%, which is conducive to the adsorption and accumulation of shale gas. Compared with the Barnett shale in the United States (Montgomery et al., 2005; Sondergeld et al., 2010), the shale samples in the study area have a higher amount of clay minerals, which is mainly related to the continental sedimentary environment.
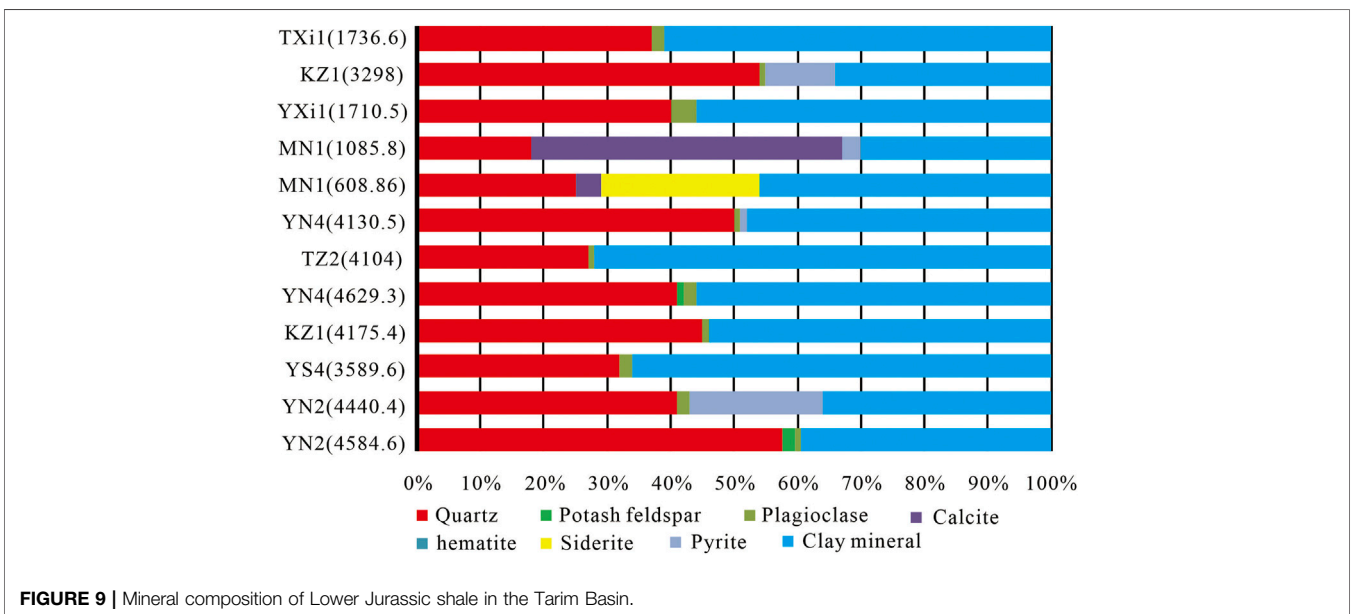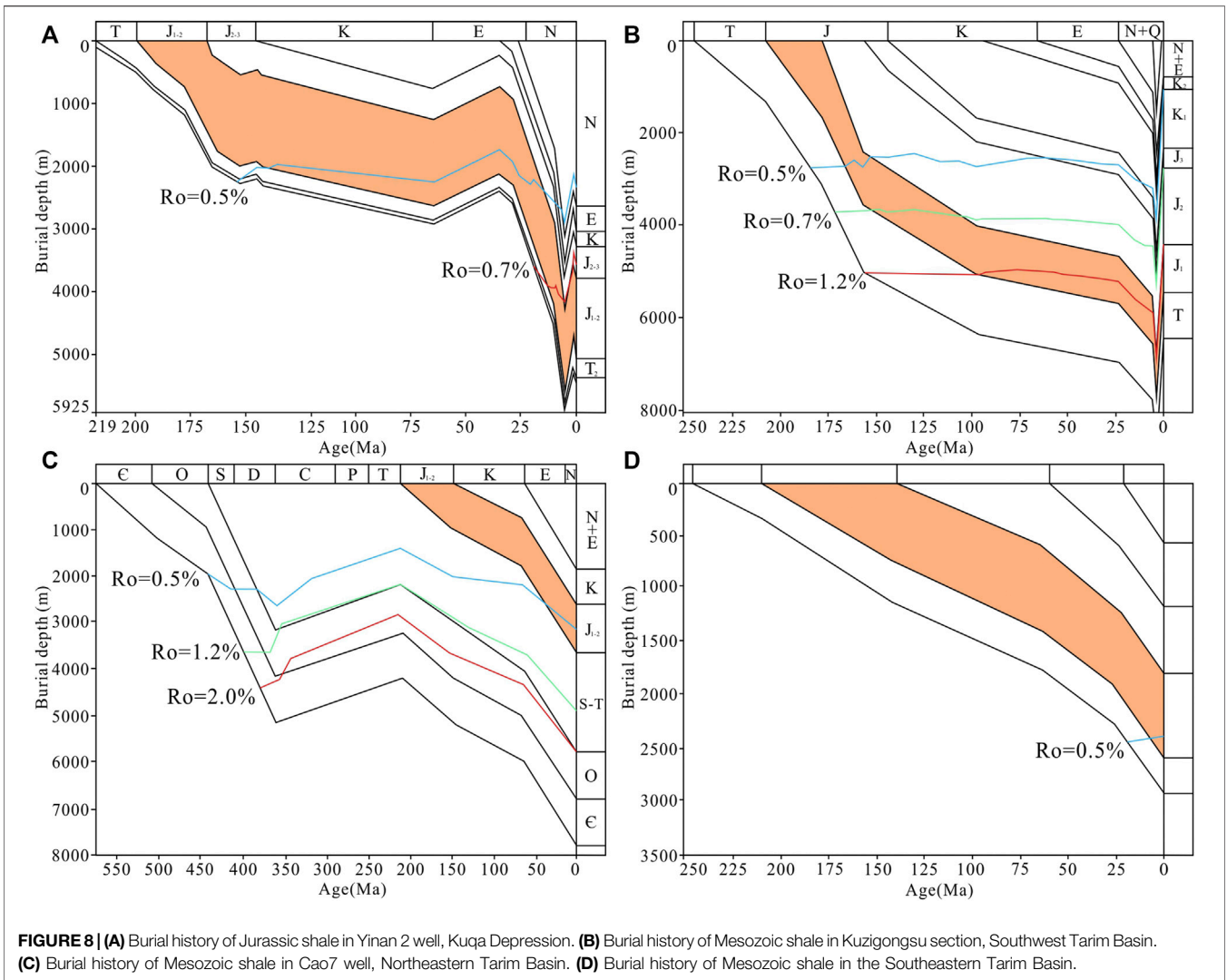
Gas Sorption Capacity

In addition to the free state of natural gas in shale in larger pores or fissures, the natural gas is also adsorbed on the surface of clay mineral particles and organic matter in a large amount (Zhang et al., 2004). In this study, the methane adsorption isotherm experiment was used to determine the adsorption isotherm of the Lower Jurassic shale in the Tarim Basin and analyze its adsorption capacity. The results show that the adsorption

isotherm test results of the shale in the study area accord with the Langmuir isotherm adsorption relationship (**Eq. 1**) (Kondo et al., 2005).

$$V = \frac{V_L P}{P_L + P} \tag{1}$$

Among them, V is the measured adsorption capacity, m^3/t; V_L is the Langmuir volume, which is the maximum adsorption capacity, m^3/t; P is the experimental pressure, MPa; and P_L is the Langmuir pressure, which is the pressure when the adsorption capacity is half of V_L.

The adsorption isotherms of different shale samples differ greatly in shape, but they are all single-molecule adsorption types; that is, the adsorption amount in the first half of the stage increases rapidly with the increase of pressure, and then the range of change becomes smaller, and the adsorption tends to be saturated. This adsorption characteristic reflects the pore structure of shale in the study area dominated by micropores and microcracks; that is, there is a large free internal surface area for adsorption in the pores or microfractures at the initial stage of the test. As the pressure increases, methane rapidly adsorbs on the surface of mineral particles and organic matter. As the adsorption progresses, the surface area of the pores not occupied by methane molecules decreases rapidly, resulting in a decrease in the adsorption increment and the curve tends to be horizontal. Specifically, the maximum adsorption capacity of shale in the study area is mainly between 0.5 and 4 m^3/t, and there are some shale samples larger than 4 m^3/t (**Figure 10**), which have high gas

FIGURE 8 | (A) Burial history of Jurassic shale in Yinan 2 well, Kuqa Depression. (B) Burial history of Mesozoic shale in Kuzigongsu section, Southwest Tarim Basin. (C) Burial history of Mesozoic shale in Cao7 well, Northeastern Tarim Basin. (D) Burial history of Mesozoic shale in the Southeastern Tarim Basin.

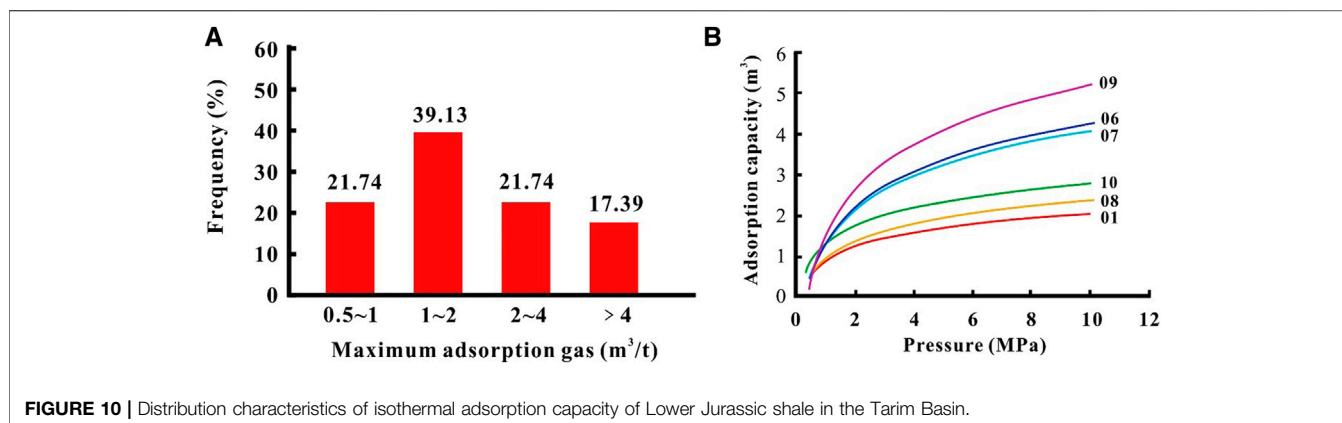FIGURE 9 | Mineral composition of Lower Jurassic shale in the Tarim Basin.

FIGURE 10 | Distribution characteristics of isothermal adsorption capacity of Lower Jurassic shale in the Tarim Basin.

TABLE 1 | Reference standard for optimization of favorable areas of continental and transitional shale gas.

Mainly parameter	Variation range
TOC(%)	Average not less than 0.5%
Ro (%)	Not less than 0.5%
Burial depth	100–4,500 m
Surface condition	Plains, hills, mountains, deserts, plateaus, etc.
Preservation condition	Development and distribution of regional shale

content. The maximum adsorbed gas volume of different shale is quite different, which is related to factors such as the abundance of organic matter, the thermal evolution maturity of organic matter and the content of clay minerals of the shale (Peng and Lian, 2017).

Favorable Exploration Areas

Based on the shale plane distribution, geochemical characteristics, and gas-bearing data, this research adopts the superposition method of main controlling geological factors to predict the prospective and favorable areas for the Lower Jurassic shale gas exploration in the Tarim Basin. The main geological factors include thickness, Ro, TOC, and top structure of Lower Jurassic shale. The evaluation parameter system of the prospective area and the favorable area are shown in **Tables 1, 2**, respectively. The results show that the Lower Jurassic shale gas prospective area of the Tarim Basin is distributed in the

Kuqa Depression, the East Tarim, and the Kashi Sag–Yecheng Sag in the Southwest Tarim. The favorable areas are mainly distributed in the Keshen and Yinan-Yeyun areas in the Kuqa Depression and the Caohu Sag-Mandong area in the East Tarim (**Figure 11**).

The shale in the Keshen favorable area in the Kuqa Depression is mainly composed of shallow-semi deep lacustrine facies. The cumulative thickness of shale with a single-layer thickness greater than 10 m is 30–100 m, and the burial depth is mainly between 3,000 and 4000 m. In mainly gray-black mudstone intercalated with argillaceous siltstone, TOC is between 2.0% and 2.5%, organic matter type is mainly type III, and the degree of thermal evolution of organic matter is low maturity–mature, with Ro between 1.25% and 1.5%. The cumulative thickness of the shale in the Yinan-Yeyun favorable area is 50–200 m, the buried depth is mainly between 3,000 and 4500 m, the TOC is between 1.5% and 3.0%, the organic matter is mainly type III, the degree of thermal evolution of the organic matter is low maturity–mature, and Ro is mostly between 0.75% and 1%. The free shale gas content is between 0.174 and 0.743 m^3/t, the adsorbed shale gas content is between 0.905 and 0.956 m^3/t, the total gas content is between 1.079 and 1.699 m^3/t, and the gas content is low.

The shale in the Caohu Sag-Mandong favorable area in East Tarim is mainly composed of shallow lake facies and floodplain facies deposits. The cumulative thickness of shale with a single-layer thickness greater than 10 m is 30–50 m, and the buried depth is mainly between 3,000 and 4000 m. In mainly

TABLE 2 | Reference standard for optimization of favorable areas of continental and transitional shale gas.

| Mainly parameter	Variation range
Lower limit of shale area	The smallest area of the target area may be found in it, and it may be distributed in the stable area or the reformed area. According to many factors, the lower shale area is 200–500 km^2
Shale thickness	The thickness of a single layer is not less than 10 m, or the ratio of mudstone thickness to stratum thickness is greater than 60. Single layer thickness is greater than 5 m and continuous is not less than 30 m
TOC (%)	1.5%–2%, average not less than 2%
Ro (%)	Type I kerogen not less than 1.2%; Type II not less than 0.7%; Type III not less than 0.5%
Burial depth	300–4,500 m
Surface condition	The terrain height difference is small, such as plains, hills, deserts, etc.
Total air content	Not less than 0.5 m^3/t
Preservation condition	Middle
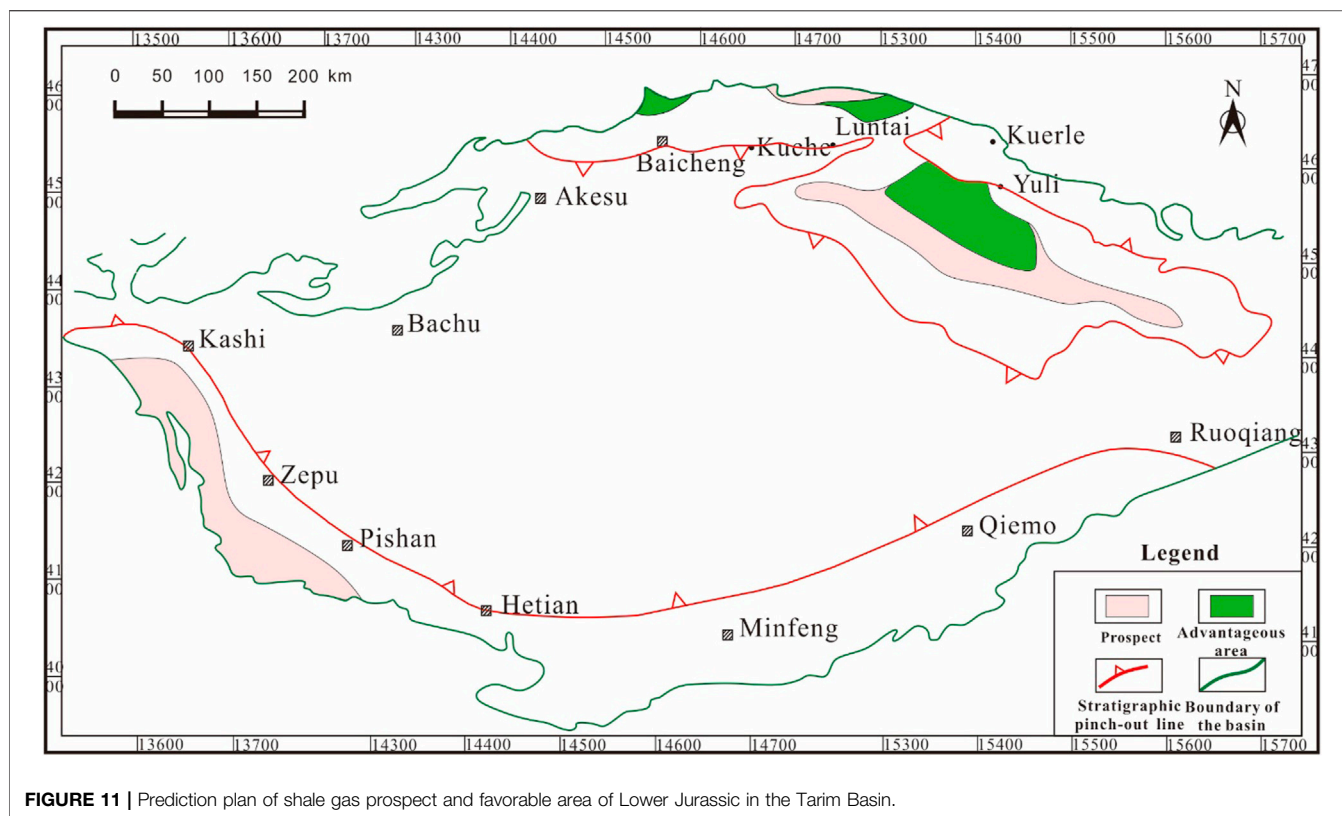
FIGURE 11 | Prediction plan of shale gas prospect and favorable area of Lower Jurassic in the Tarim Basin.

carbonaceous mudstone and silty mudstone, TOC is between 1.5% and 2.5%, organic matter type is mainly type III, and the degree of thermal evolution of organic matter is low maturity–mature, with Ro mostly between 0.5% and 1.0%. The free shale gas content ranges from 0.703 to 1.654 m^3/t, the adsorbed shale gas content ranges from 0.792 to 0.986 m^3/t, and the total gas content ranges from 1.495 to 2.640 m^3/t. The gas content is relatively high.

The shale in the Kashgar Sag–Yecheng Sag prospective area in Southwest Tarim is mainly fluvial-marsh deposits. The cumulative thickness of shale with a single-layer thickness of more than 10 m is 30–100 m, and the burial depth is mainly between 2,000 and 4,000 m and the TOC is between 0.5% and 1.5%. Due to the low abundance of organic matter in shale, there is no favorable area for shale gas exploration in the Southwest Tarim.

Based on the above analysis, the Lower Jurassic shale gas in the Tarim Basin has good prospects for exploration, and the Caohu Sag-Mandong area in the East Tarim is the most advantageous.

CONCLUSION

1) The Lower Jurassic shale in the Tarim Basin is mainly distributed in the Kuqa Depression, East Tarim Basin, and Southwest Tarim Basin. The deposition thickness center is located in the Yangxia Sag of the Kuqa Depression and the Kashi Sag and Yecheng Sag of the Southwest Tarim Basin. The maximum thickness is respectively 200 and 100 m. The TOC of the Lower Jurassic

shale is higher overall, of which the TOC of the shale in the Baicheng Sag–Yangxia Sag in the Kuqa Depression exceeds 3%; the TOC of the shale in the East Tarim Basin area is more than 1%. The high values are mainly located in the Caohu Sag-Mandong area and Yingjisu Sag; some shale in the Southwest Tarim Basin have TOC greater than 1.5%. Organic matter is mainly type III kerogen, followed by type II_2 kerogen, and type II_1 and type I kerogen are basically underdeveloped. The thermal evolution maturity of organic matter is relatively high in the Baicheng Sag of the Kuqa Depression, and Kashgar and Yecheng Sag of the Southwest Tarim Basin, of which Ro is more than 2%, and it is in the high-over-mature evolution stage. The thermal degree of evolution is relatively low due to the relatively shallow buried depth, and Ro is mostly less than 1%. The mineral composition of shale is dominated by brittle minerals such as quartz and clay minerals. The content of brittle minerals is more than 40%, which is conducive to the later fracturing development; the content of clay minerals is more than 40%, which is conducive to the adsorption and accumulation of shale gas. The maximum adsorbed gas volume of shale is mainly between 0.5 and 4 m^3/t, and shale larger than 4 m^3/t also exists with high gas content.

2) The Lower Jurassic shale gas prospective area of the Tarim Basin is distributed in the Kuqa Depression, the East Tarim Basin, and the Kashi Sag–Yecheng Sag in the Southwest Tarim Basin. The favorable areas are mainly distributed in the Keshen and Yinan-Yeyun region of the Kuqa Depression and the Caohu Sag-Mandong region of the East Tarim Basin.

DATA AVAILABILITY STATEMENT

The original contributions presented in the study are included in the article/Supplementary Material, further inquiries can be directed to the corresponding authors.

AUTHOR CONTRIBUTIONS

QW: Study design, Research, Data analysis, and Writing—original draft. HT: Data curation, Methodology, Formal analysis, Writing—original draft, and Writing—review and editing. ZG: Idea refinement and Manuscript revision. GC: Data curation, Investigation, and Formal analysis. ZL: Writing—review and editing. QL: Writing—review and editing.

FUNDING

REFERENCES

Chen, J., Zhao, C., Wang, Z., He, Z., and Qin, Y. (1998). Organic Geochemical Characteristics of Oil, Gas and Source Rocks of Jurassiccoal Measures in Northwestern China. *Geol. Rev.* 44 (2), 149–159. doi:10.3321/j.issn:0371-5736.1998.02.006

Gao, X., Liu, L., Shang, X., Wang, Y., and Su, T. (2013). Characterization of Jurassic Shale Reservoirs and the Geological Background of Shale Gas Accumulations in Tarim Basin. *Acta Petrol. Sin.* 34 (4), 647–659. doi:10.7623/syxb201304004

Gao, X. Y., Liu, L. F., Jiang, F. J., Wang, Y., Xiao, F., Ren, Z. Y., et al. (2015). Analysis of Geological Effects on Methane Adsorption Capacity of Continental Shale: A Case Study of the Jurassic Shale in the Tarim Basin, Northwestern China. *Geol. J.* 51 (6), 936–948. doi:10.1002/gj.2706

Haikuan, N., Jinchuan, Z., and Yuxi, L. (2011). Accumulation Conditions of the Lower Cambrian Shale Gas in the Sichuan Basin and its Periphery. *Acta Petrolei Sinica* 32 (6), 959–967.

He, D., Jia, C., Li, D., Zhang, C., Meng, Q., and Shi, X. (2005). Formation and Evolution of Polycyclic Superimposed Tarim basin. *Oil& Gas Geology.* 26 (1), 64–77. (in Chinese). doi:10.3321/j.issn:0253-9985.2005.01.010

Hopkins, A. S. (2017). The Next Energy Economy. *Science* 356 (6339), 709. doi:10.1126/science.aam8696

Hu, T., Pang, X., Jiang, F., Wang, Q., Liu, X., Wang, Z., et al. (2021). Movable Oil Content Evaluation of Lacustrine Organic-Rich Shales: Methods and a Novel Quantitative Evaluation Model. *Earth-Science Rev.* 214, 103545. doi:10.1016/j.earscirev.2021.103545

Hu, T., Pang, X., Jiang, S., Wang, Q., Xu, T., Lu, K., et al. (2018). Impact of Paleosalinity, Dilution, Redox, and Paleoproductivity on Organic Matter Enrichment in a Saline Lacustrine Rift Basin: A Case Study of Paleogene Organic-Rich Shale in Dongpu Depression, Bohai Bay Basin, Eastern China. *Energy Fuels* 32 (4), 5045–5061. doi:10.1021/acs.energyfuels.8b00643

Hu, T., Pang, X. Q., Yu, S., Wang, X., Pang, H., Guo, J., et al. (2016). Hydrocarbon Generation and Expulsion Characteristics of Lower Permian P1f Source Rocks in the Fengcheng Area, Northwest Margin, Junggar Basin, NW China: Implications for Tight Oil Accumulation Potential Assessment. *Geol. J.* 51, 800–890. doi:10.1002/gj.2705

Hughes, J. D. (2013). Energy: a Reality Check on the Shale Revolution. *Nature* 494 (7437), 307. doi:10.1038/494307a

Jia, C. (1997). *The Structural Characteristics and Hydrocarbon of the Tarim Basin in China*. Beijing: Petroleum Industry Press.

Jiang, F., Chen, J., Xu, Z., Wang, Z., Hu, T., Chen, D., et al. (2017). Organic Matter Pore Characterization in Lacustrine Shales with Variable Maturity Using Nanometer-Scale Resolution X-Ray Computed Tomography. *Energy Fuels* 31 (3), 2669–2680. doi:10.1021/acs.energyfuels.6b03313

Jiang, F., Pang, X., Ouyang, X., Guo, J., Jin, C., Huo, Z., et al. (2012). The Main Progress and Problems of Shale Gas Study and the Potential Pre-diction of Shale Gas Exploration. *Earth Sci. Front.* 19 (2), 198–211.

Jiang, F. J, Hu, T., Liu, L., Wang, Q., Gao, X., Zhang, P., et al. (2019). Geochemical and Geological Characteristics of the Jurassic Continental Black Shale in the Southwestern Depression of Tarim Basin. *Geol. J.* 54 (3), 1115–1131. doi:10.1002/gj.3212

Jiang, F. J., Wang, Q., Liu, L., Gao, X., and Hu, T. (2018). Geological and Geochemical Characteristics of the Middle–Lower Jurassic Shales in the Kuqa Depression, Tarim Basin: An Evaluation of Shale Gas Resources. *Austral. J. Earth Sci.* 65 (4), 557–573. doi:10.1080/08120099.2018.1447014

Kondo, S., Ishikawa, D., and Abe, K. (2005). *Adsorption science[M] Translated by Li Guoxi*. Beijing: Chemical Industry Press.

Li, C., Wang, L., Guo, S., and Shi, X. (2000). Geothermal Evolution in Tarim Basin. *Acta petrologica Sinica* 03, 13–17+107.

Loucks, R. G., and Ruppel, S. C. (2007). Mississippian Barnett Shale: Lithofacies and Depositional Setting of a Deep-Water Shale-Gas Succession in the Fort Worth Basin, Texas. *Bulletin* 91 (4), 579–601. doi:10.1306/11020606059

Montgomery, S. L., Jarvie, D. M., Bowker, K. A., and Pollastro, R. M. (2005). Mississippian Barnett Shale, Fort Worth basin, north-central Texas: Gas-Shale Play with Multi-Trillion Cubic Foot Potential. *Bulletin* 89 (2), 155–175. doi:10.1306/09170404042

Pan, J., and Hu, J. (2020). Study on Sedimentary System of Kuqa Depression in Tarim Basin. *Contemp. Chem. industry* 49 (10), 2264–2267. doi:10.3969/j.issn.1671-0460.2020.10.038

Peng, W., and Lian, Y. (2017). Discussion on Influencing Factors of Shale Gas Content in continental Sedimentary basin: a Case Study of Weibei Sag. *Shandong land Resour.* 33 (07), 25–30.

Peters, K. E., and Cassa, M. R. (1994). "Applied Source Rock Geochemistry," in *The Petroleum System: From Source to Trap*. Editors L.B. Magoon and W.G. Dow (Tulsa: American Association of Petroleum Geologists), 93–120.

Pu, B., Jiang, Y., Wang, Y., Bao, S., and Liu, X. (2010). Reservoir-forming Conditions and Favorable Exploration Zones of Shale Gas in Lower Silurian Longmaxi Formation of Sichuan Basin. *Acta Petrolei Sinica* 31 (2), 225–230.

Qiu, N., Zuo, Y., Chang, J., Xu, W., and Zhu, C. (2015). Characteristics of Meso-Cenozoic thermal Regimes in Typical Eastern and Western Sedimentary Basins of China. *Earth Sci. Front.* 22 (1), 157–168. doi:10.13745/j.esf.2015.01.013

Sondergeld, C. H., Newsham, K. E., Rice, M. C., and Rai, C. S. (2010). *Petrophysical Considerations in Evaluating and Producing Shale Gas Resources*. Pittsburgh, USA: SPE.

Tang, L., Wan, G., Wang, Q., Jin, W., and Yang, W. (2008). Mesozoic and Cenozoic Tectonic Evolution of the West Churtag Tectonic belt, Kuche. *J. Southwest Pet. Univ. (Natural Sci. edition)* 02, 167–171+201.

Tissot, B. P., and Welte, D. H. (1984). *Petroleum Formation and Occurrence*. New York: Springer-Verlag.

Wang, L., Li, C., Liu, S., and Li, H. (2002). "Geothermal Field and Cenozoic thermal Regime in Kuqa Depression," in 2002-Proceedings of the 18th annual meeting of the Chinese Geophysical Society (Beijing, China: Chinese Geophysical Society), 1. Chinese Geophysical Society. Annual journal of the Chinese Geophysical Society.

Wang, Z., Tian, J., Wang, Q., Pi, X., Wang, G., Li, Y., et al. (2004). *Oil and Gas Exploration and Practice in Tarim Basin*. Beijing: Petroleum Industry Press. (in Chinese).

Xiao, F., Liu, L., Zhang, Z., Wu, K., Xu, Z., and Zhou, C. (2014). Conflicting Sterane and Aromatic Maturity Parameters in Neogene Light Oils, Eastern Chepaizi

High, Junggar Basin, NW China. *Org. Geochem.* 76, 48–61. doi:10.1016/j. orggeochem.2014.07.014

Zhang, J., Jin, Z., and Yuan, M. (2004). Accumulation Mechanism and Distribution of Shale Gas. *Nat. gas industry* 24 (07), 15-18+131–132. doi:10.3321/j.issn:1000-0976.2004.07.005

Zhang, L., Jiang, Z., and Guo, Z. (2007). Relationship between Structural Stress and Hydrocarbon Bearing Pool Formation. *Nat. Gas Geosci.* 18 (1), 32–36. doi:10.3969/j.issn.1672-1926.2007.01.004

Zhao, M., and Zhang, B. (2002). Source Rocks for a Giant Gas Accumulating Area in the Kuqa Foreland Depression. *Sci. Geol. Sin.* 45 (S1), 35–44. doi:10.3321/j. issn:0563-5020.2002.z1.005

Zou, C., Dong, D., Wang, S., Li, J., Li, X., Wang, Y., et al. (2010). Geological Characteristics, Formation Mechanism and Resource Potential of Shale Gas in China[J]. *Pet. Exploration Develop.* 37 (6), 641–653.

Zou, C. N. (2017). *Unconventional Petroleum Geology*. Amsterdam, Netherlands: Elsevier.